NANO LETTERS

2002
Vol. 2, No. 10
1177−1181

Control of Multiwalled Carbon Nanotube Diameter by Selective Growth on the Exposed Edge of a Thin Film Multilayer Structure

Nitin Chopra,[†] Padmakar D. Kichambare,[‡] Rodney Andrews,[‡] and Bruce J. Hinds*,[†]

Department of Chemical and Materials Engineering, University of Kentucky, Lexington, Kentucky 40506-0046, and Center for Applied Energy Research, University of Kentucky, Lexington, Kentucky 40511-8410

Received July 16, 2002; Revised Manuscript Received August 12, 2002

ABSTRACT

Selective area growth of carbon nanotubes (CNT) has been used to control the diameter of CNTs. Narrow lines of SiO_2 (12–60 nm) are formed at the cleaved face of a $Si/SiO_2/Si$ multilayer structure. CNTs are then grown by a chemical vapor deposition process with a ferrocene/xylene/H_2/Ar mixture at 700 °C. CNTs are observed to grow only on the exposed SiO_2 surface at the edge of the "mesa" structure with a diameter equal to the thickness of the SiO_2 layer.

Carbon nanotubes (CNTs) have been demonstrated to be the basis of several key device applications in electronics,[1−3] sensors,[4] and nanoelectromechanical systems (NEMS).[5] The advantages of incorporating CNTs include high functional density, low power consumption, and the potential for selective chemical modification. Particularly intriguing is that, due to the long length of tubes, it is possible to use commercially prevalent micron scale lithography to result in nm-scale line features if one can selectively incorporate CNTs. Thus the development of a method to control CNT diameter and its placement becomes critical for applications. A particularly promising study has shown that it is possible to bridge the tops of photolithographically defined "posts" with CNTs grown from nanoscale catalyst support particles.[6,7] With this technique CNTs are grown in all directions, but those that do not bridge the gap between posts fall to the side. Further refinements of the concept of growing CNTs between photolithographically defined pillars could become the basis of nm-scale thin wiring. There are a variety of growth techniques for CNT synthesis such as arc discharge, CVD, laser ablation, and template assisted growth.[8,9] The CVD method offers the most commercially viable technique due to a large uniform reaction area and high mass flux flows.[10−13] In all growth techniques, the CNT diameter is determined largely by the size of the nm-scale catalyst particle.[14−16] These catalysts can be metal particles[17] or a coating of transition metal on catalyst support particles.[18,19] Thus, to control CNT diameter there is a significant challenge to control colloid size dispersion, and there are promising reports to this end.[20,21] However, it remains a challenge to place only a few nanoparticles in predefined locations without agglomeration of nanoparticles or coarsening.[22] Catalytic nanoparticles can be supplied during growth in a xylene- and ferrocene-based CVD process. This process can grow CNTs at high densities with noteworthy vertical alignment.[11] The diameter of resultant CNTs is a complicated system that involves the surface free energy of catalyst and substrate, surface migration, and ferrocene decomposition rates. Under a certain temperature and xylene and ferrocene feed rate it is possible determine CNT diameter in the range of 30−100 nm with a dispersion approximately 30%.[14] Importantly, CNT growth with the ferrocene-catalyzed CVD process can be selective to substrate composition.[23−26] In particular, these surfaces can be easily patterned by conventional microprocessing, resulting in predetermined lines of vertically aligned dense arrays of CNT "forests". The H-terminated Si surface will not grow CNTs, while a SiO_2 surface will in this xylene/ferrocene CVD process.[24] Because of the limitation of conventional lithography in the near-micron regime, it is not known if the resultant CNT diameter could actually be determined by line width of an SiO_2 surface. By using the exposed edged of a thin film multilayer structure with a 10−60 nm thick SiO_2 layer, we demonstrate that CNT diameter

* Corresponding author. E-mail: bjhinds@engr.uky.edu
[†] Department of Chemical and Materials Engineering.
[‡] Center for Applied Energy Research.

10.1021/nl0257061 CCC: $22.00 © 2002 American Chemical Society
Published on Web 08/30/2002

Scheme 1. Synthetic Steps for the Growth of Carbon Nanotubes from Exposed Face of $Si/SiO_2/Si$ Multilayer[a]

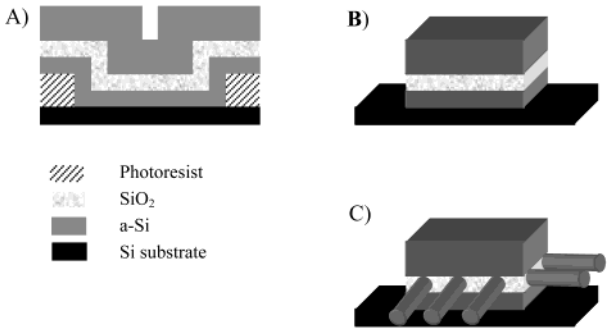

[a] (A) cross-section of photo resist pattern with e-beam evaporated $Si/SiO_2/Si$ multilayer. Figure is not drawn to scale as film thickness is ~100 nm total while pattern is ~100 um square. (B) Post structure after photo resist liftoff and HF etching of surface oxide. (C) CNT growth on exposed face of SiO_2 thin film.

can be controlled in a CVD growth process. Importantly, this CNT diameter is determined by thin film thickness of SiO_2, which is easily controlled by conventional semiconductor processing. These CNTs can be used directly in wiring between post structures or harvested into solution for later self-assembly processes.

The experimental steps of controlled CNT growth from the exposed edge of a $Si/SiO_2/Si$ multilayer are outlined in Scheme 1. A cleaned silicon wafer (International Wafer Service, B doped 12 ohm cm^{-1} ⟨100⟩) was patterned using photolithography. The silicon wafer surface was spin coated with positive photo resist (Microposit S1813 positive photo resist, Shipley). This was exposed in mask aligner (KARL-SUSS MJB3) with a test pattern mask of 100, 30, 10, and 5 um square holes. After developing the pattern on the silicon wafer surface, a thin film multilayer structure was deposited over the photoresist pattern by employing a four-pocket e-beam evaporation system with a background pressure of 10^{-6} Torr (Thermionics Laboratory). The bottom amorphous Si (a-Si) layer was 40−100 nm, middle SiO_2 layer 12−65 nm thick, and top a-Si layer 50−60 nm thick as monitored by crystal quartz monitor during evaporation. The sample is then immersed in boiling acetone for 2 min 30 s to lift of the photo resist and material above, resulting in an array of post structures. Each post has exposed edges of $Si/SiO_2/Si$ layers, as in a mesa structure. An important experimental subtlety is that the bottom a-Si layer is required because the "liftoff" process does not result in a perfect break at the substrate. A relatively large and uncontrolled area of SiO_2 would be exposed if only a Si/SiO_2 bilayer was used. Immediately prior to CNT growth HF (16 volume %, J. T. Baker Ltd), etching of the post structure on patterned substrate is require so as to remove any native oxide from Si exposed to atmosphere. HF etch time was limited to the time when substrate was observed to become hydrophobic. The time duration of HF etch is minimized to reduce undercutting of middle SiO_2 layer. Finally, the MWNTs were grown on samples by pyrolysis of xylene and ferrocene mixture under Ar/H_2 atmosphere in a tubular furnace as described by Andrews et al.[11] Approximately 6.5 mol % of ferrocene

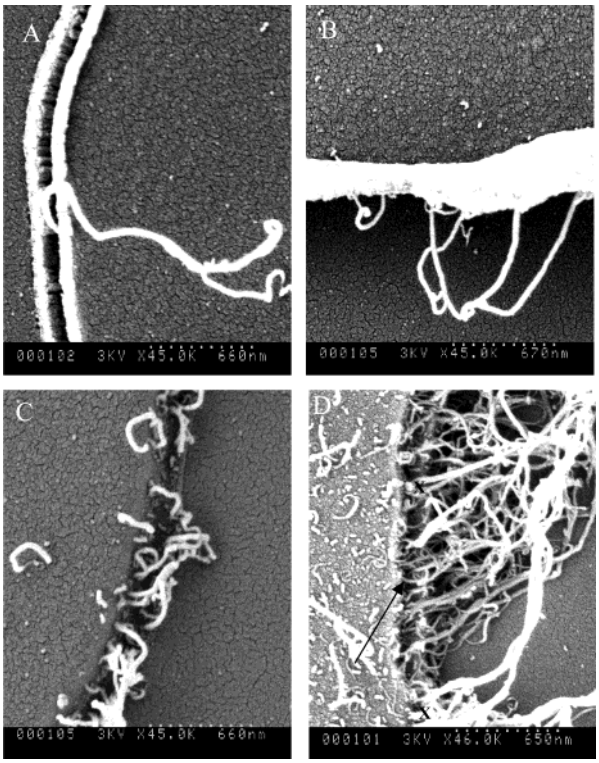

Figure 1. Scanning electron microscope image of CNT growth from exposed edge of a $Si/SiO_2/Si$ multilayer structure. SiO_2 interlayer film thickness: (A) 65 nm, (B) 19 nm, (C) 17 nm, (D) 12 nm. In Figure 1C−D, tilt angle is 40°. For statistical analysis, the arrow in 1D shows the step edge (top to bottom of image) from which every visible CNTs diameter is measured directly at their root. The crossed mark (X) shows artifacts that are eliminated from statistical analysis due to SEM charging, defects, or intertwined CNTs.

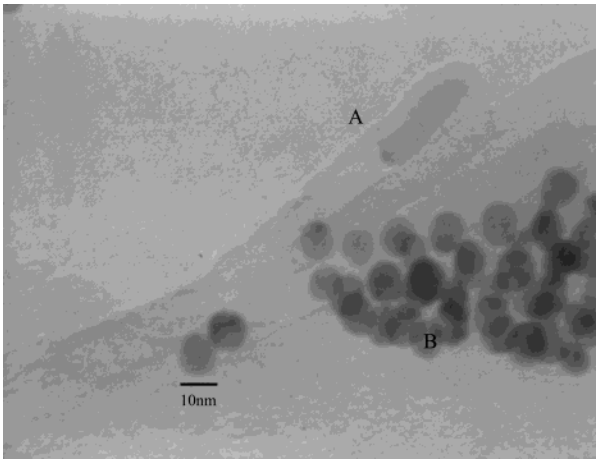

Figure 2. Transmission electron microscope image of CNT (A) from sample imaged in Figure 1D. Apparent is the multiwalled nature as well as the Fe catalyst size consistent with CNT diameter. CNT was removed from substrate by ultrasonication onto a C-coated TEM grid. Dark spherical particles are 10 nm diameter nc-Au standards (B).

(Aldrich) was dissolved in xylene (Fisher Scientific) and continuously fed into the reactor. The liquid feeding mixture was passed through a capillary tube and preheated to 175 °C prior to its entry into the furnace. At this temperature, the liquid exiting the capillary tube was immediately volatil-

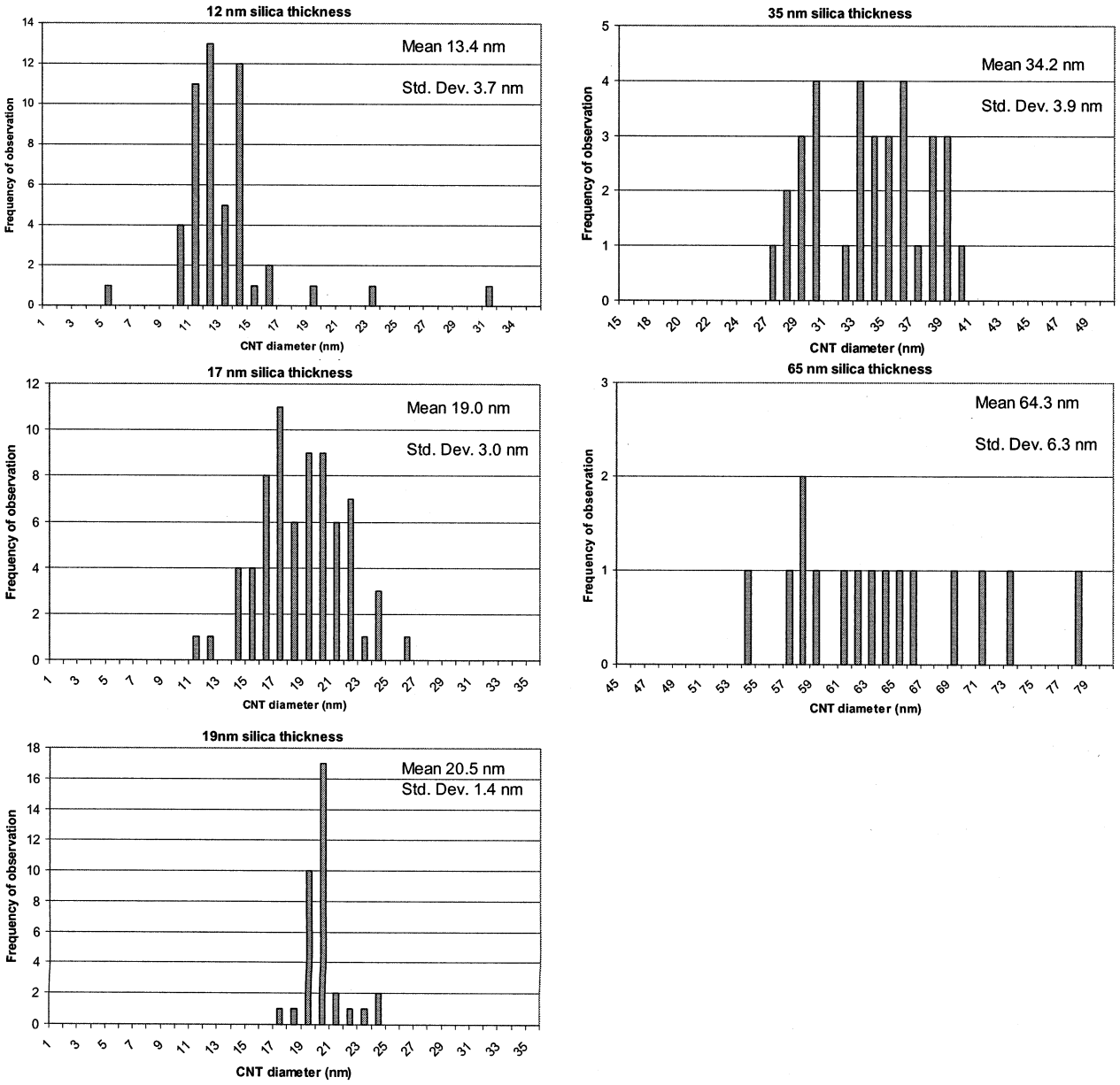

Figure 3. Histogram of observed CNT diameter by SEM as a function of SiO_2 layer thickness. Frequency of observation is shown at increments of 1 nm. Shown is the average and standard deviation for a Gaussian distribution.

ized and swept into the reaction zone of the furnace at 700 °C by the flow of argon with 10% hydrogen. Growth times were 30 min. After the reaction, the furnace was allowed to cool to room temperature in flowing argon. The microstructure of resultant CNT growth was characterized by SEM (Hitachi S900 field emission electron source with sub-nm resolution). Diameters were measured at the roots of CNT growth at the pattern edge to ensure proper depth of field focus. CNTs that originated from defect sites, multiple entangled CNTs, and areas of electron imaging charging were excluded from statistical analysis. A sub-nm thin film of Pd/Au was sputtered over the sample to reduce charging for SEM analysis. TEM analysis was performed with a JEOL JEM-2000FX. TEM sample was prepared from the ultrasonic removal of CNTs from the substrate and "floated" onto an a C-coated TEM grid.

Figure 1 shows resulting CNT growth from post edges. As expected, there is growth from pattern edges where there is exposed SiO_2 and no growth on surface hydrogen terminated Si (Si−H). In a few samples, small amounts of CNTs are seen to grow on Si−H surface. This is likely a result of slight HF underetch and background O_2 in a-Si evaporation process. The HF under/over etching can also give variability in CNT density and growth rate (as is observed in Figure 1A−D) under nominally identical growth conditions. The liftoff process can result in a tearing of the film as seen in Figure 1B, but the three-layer structure ensures that only a narrow line is exposed. Figure 2 shows a TEM image of an isolated CNT taken from the same sample as Figure 1D. A multiwalled CNT with diameter of 12 nm is seen consistent with SEM observation. Other CNT diameters observed by TEM (5 total) give an average diameter of

12.4±0.9 nm; however, SEM observations are statistically more numerous and are known to have originated from the pattern edge. The catalyst particle is of the same diameter as the CNT, as had been observed with previous TEM studies of this CVD growth process.[11,14] The catalyst particle appears to be at the tip of the CNT, as there is an encapsulating layer of a−C. This would be consistent with other studies; however, we cannot rule out the possibility that the present amorphous layer is an artifact of TEM sample preparation. Figure 3 shows the resultant CNT diameter as a function of SiO_2 layer thickness from SEM observations of Figure 1 and numerous other micrographs (not shown). Remarkable control of CNT diameter was achieved with conventional film growth techniques with a strong correlation to observed diameter to SiO_2 film thickness. This is presumably a result of the selective chemical decomposition ferrocene only on the oxide surface. Other factors may include surface migration and nucleation of Fe particles only on the oxide; however, the exact mechanism is not studied here in this communication. The observed standard deviation is significantly smaller that growth over large area SiO_2 surface but may determined by inherent to Fe nucleation kinetics or variability in SiO_2 thickness from e-beam evaporation process. Si thermal oxidation would result in improved thickness control, but high temperatures are not compatible with current liftoff process. The CNT growth conditions are essentially identical to previously reported 28-35 nm diameter CNTs;[11] however, in the 65 nm thick SiO_2 case larger (∼65 nm) CNTs are observed. This is likely the result of higher ferrocene catalyst concentration in the gas phase depletion region, resulting in larger catalyst particles. Higher catalyst concentration could be attributed to significantly reduced surface area for the decomposition reaction, higher ferrocene surface migration across H-terminated Si regions, or slight variations in process conditions. The use of an exposed edge of a multilayer structure is a highly scalable process that works well with the stable Si/SiO_2 system. There is one report of using an edge of a catalytic SiO_2/metal/SiO_2 multilayer structure (50−100 nm thick metal layer) to grow CNTs; however, there was significant metal migration at deposition conditions that destroyed any control of catalytic metal thickness.[27] Future work is to find lower limits of CNT diameter using thermal oxides for finer control by SiO_2 layer thickness. Finer control of multilayer edges would be expected by reactive ion etching (RIE) of patterns (with conditions of nearly identical Si/SiO_2 etching rates) or ion milling. In principle, the diameter of CNTs can be reduced to the 1−2 nm film thickness of oxide; however, the minimum Fe nanoparticle sizes from ferrocene decomposition conditions need to be determined.

In conclusion we have demonstrated that the diameter of CNTs has been controlled by line width of reactive SiO_2 surface in a ferrocene/xylene CVD process. The resulting structure can be used for nanowiring or lithographic processes.[28] Alternatively CNTs can be "harvested" from dense arrays of post patterns and used for later self-assembly processes. The use of an exposed edge is a readily achievable process to make nm-wide lines. This technique can be readily applied to other selective growth systems or self-assembly chemistry as a general tool in nanofabrication.

Acknowledgment. The authors thank the NSF-MERSEC Advanced Carbon Materials Center (DMR-9809686) as well as sponsorship by the Air Force Research Laboratory (DEPSCoR program) under agreement number F49620-02-1-0225. The authors also appreciate the use of university fabrication (CMMED) and microscopy facilities, with particular thanks to Dr. Alan Dozier for help with TEM observation.

References

(1) Bachtold, A.; Hadley, P.; Nakanishi, T.; Dekker, C. Logic Circuits with Carbon Nanotube Transistors; *Science* **2001**, *294*, 1317.
(2) Tsukagoshi, K.; Alphenaar, B. W.; Ago, H. Coherent transport of electron spin in a ferromagnetically contacted carbon nanotube; *Nature* **1999**, *401*, 572−574.
(3) Liu, K.; Avouris, Ph.; Martel, R.; Hsu, W. K. 'Electrical transport in doped multiwalled carbon nanotubes; *Phys. Rev. B* **2001**, *6316*, art. no.-161404.
(4) Chang, H.; Lee, J. D.; Lee, S. M.; Lee, Y. H. Adsorption of NH_3 and NO_2 molecules on carbon nanotubes; *Appl. Phys. Lett.* **2001**, *79*, 3863−3865.
(5) Williams, P. A.; Papadakis, S. J.; Falvo, M. R.; Patel, A. M.; Sinclair, M.; Seeger, A.; Helser, A.; Taylor, R. M.; Washburn, S.; Superfine, R. Controlled placement of an individual carbon nanotube onto a microelectromechanical structure; *Appl. Phys. Lett.* **2002**, *80*, 2574−2576.
(6) Cassell, A. M.; Franklin, N. R.; Tombler, T. W.; Chan, E. M.; Han, J.; Dai, H. J. Directed growth of free-standing single-walled carbon nanotubes; *J. Am. Chem. Soc.* **1999**, *121*, 7975−7976.
(7) Franklin, N. R.; Dai, H. J. An enhanced CVD approach to extensive nanotube networks with directionality; *Adv. Mater.* **2000**, *12*, 890−894.
(8) For a detailed review see Huczko, A. Synthesis of aligned carbon nanotubes; *Appl. Phys. A* **2002**, *74*, 617−638.
(9) Dai, H. J.; Kong, J.; Zhou, C. W.; Franklin, N.; Tombler, T.; Cassell, A.; Fan, S. S.; Chapline, M. Controlled chemical routes to nanotube architectures, physics, and devices' *J. Phys. Chem. B* **1999**, *103*, 11246−11255.
(10) Terrones, M.; Grobert, N.; Olivares, J.; Zhang, J. P.; Terrones, H.; Kordatos, K.; Hsu, W. K.; Hare, J. P.; Townsend, P. D.; Prassides, K.; Cheetham, A. K.; Kroto, H. W.; Walton, D. R. M. Controlled production of aligned-nanotube bundles; *Nature* **1997**, *388*, 52−55.
(11) Andrews, R.; Jacques, D.; Rao, A. M.; Derbyshire, F.; Qian, D.; Fan, X.; Dickey, E. C.; Chen, J. Continuous production of aligned carbon nanotubes: a step closer to commercial realization' *Chem. Phys. Lett.* **1999**, *303*, 467−474.
(12) Cassell, A. M.; Raymakers, J. A.; Kong, J.; Dai, H. J. Large scale CVD synthesis of single-walled carbon nanotubes; *J. Phys. Chem. B* **1999**, *103*, 6484−6492.
(13) Che, G.; Lakshmi, B. B.; Martin, C. R.; Fisher, E. R.; Ruoff, R. S. Chemical vapor deposition based synthesis of carbon nanotubes and nanofibers using a template method *Chem. Mater.* **1998**, *10*, 260−267.
(14) Sinnott, S. B.; Andrews, R.; Qian, D.; Rao, A. M.; Mao, Z.; Dickey, E. C.; Derbyshire, F. Model of carbon nanotube growth through chemical vapor deposition; *Chem. Phys. Lett.* **1999**, *315*, 25−30.
(15) Cheung, C. L.; Kurtz, A.; Park, H.; Lieber, C. M.; Diameter controlled synthesis of carbon nanotubes; *J. Phys. Chem. B* **2002**, *106*, 2429−2433.
(16) Kukovitsky, E. F.; L'vov, S. G.; Sainov, N. A.; Shustov, V. A.; Chernozatonskii, L. A. Correlation between metal catalyst particle size and carbon nanotube growth; *Chem. Phys. Lett.* **2002**, *355*, 497−503.
(17) Ho, G. W.; Wee, A. T. S.; Lin, J.; Tjiu, W. C. Synthesis of well-aligned multiwalled carbon nanotubes on Ni catalyst using radio frequency plasma-enhanced chemical vapor deposition; *Thin Solid Films* **2001**, *388*, 73−77.
(18) Hernadi, K.; Fonseca, A.; Nagy, J. B.; Bernaerts, D.; Fudala, A.; Lucas, A. A. Catalytic synthesis of carbon nanotubes using zeolite support; *Zeolites* **1996**, *17*, 416−423.

(19) Hernadi, K.; Fonseca, A.; Piedigrosso, P.; Delvaux, M.; Nagy, J. B.; Bernaerts, D.; Riga, J. Carbon nanotubes production over Co/silica catalysts; *Catal. Lett.* **1997**, *48*, 229−238.
(20) Ago, H.; Komatsu, T.; Ohshima, S.; Kuriki, Y.; Yumura, M. 'Dispersion of metal nanoparticles for aligned carbon nanotube arrays' *Appl. Phys. Lett.* **2000**, *77*, 79−81.
(21) Li, Y.; Liu, J.; Wang, Y. Q.; Wang, Z. L. Preparation of monodispersed Fe−Mo nanoparticles as the catalyst for CVD synthesis of carbon nanotubes; *Chem. Mater.* **2001**, *13*, 1008−1014.
(22) Jost, O.; Gorbunov, A. A.; Moller, J.; Pompe, W.; Graff, A.; Friedlein, R.; Liu, X.; Golden, M. S.; Fink, J. Impact of catalyst coarsening on the formation of single-wall carbon nanotubes; *Chem. Phys. Lett.* **2001**, *339*, 297−304.
(23) Wei, B. Q.; Zhang, Z. J.; Ajayan, P. M.; Ramanath, G. Growing pillars of densely packed carbon nanotubes on Ni-coated silica; *Carbon* **2002**, *40*, 47−51.
(24) Wei, B. Q.; Vajtai, R.; Jung, Y.; Ward, J.; Zhang, R.; Ramanath, G.; Ajayan, P. M. Organized assembly of carbon nanotubes − Cunning refinements help to customize the architecture of nanotube structures' *Nature* **2002**, *416*, 495−496.
(25) D. Qian Ph.D. Dissertation, University of Kentucky, 2001
(26) Rao, A. M.; Jacques, D.; Haddon, R. C.; Zhu, W.; Bower, C.; Jin, S. In Situ Grown Carbon Nanotube Array with Excellent Field Emission Characteristics; *Appl. Phys. Lett.* **2000**, *76*, 3813.
(27) Han, Y. S.; Shin, J. K.; Kim, S. T. Synthesis of carbon nanotube bridges on patterned silicon wafers by selective lateral growth; *J. Appl. Phys.* **2001**, *90*, 5731−5734.
(28) Lefebvre, J.; Radosavljevic, M.; Johnson, A. T. Fabrication of nanometer size gaps in a metallic wire; *Appl. Phys. Lett.* **2000**, *76*, 3828−3830.

NL0257061